An Efficient Propagation Model for Automatic Planning of Indoor Wireless Networks

Antonis G. Dimitriou[#], Stavroula Siachalou[#], Aggelos Bletsas[+], John N. Sahalos[*]

[#]*Department of Electrical & Computer Engineering, Aristotle University of Thessaloniki*
AUTh Campus,ECE Dept., 54124, Thessaloniki, Greece
antodimi@ee.auth.gr, ssiachal@auth.gr

[+]*Department of Electronic & Computer Engineering, Technical University of Crete*
TUC Campus, Kounoupidiana, 73100, Chania, Greece
aggelos@telecom.tuc.gr

[*]*Physics Department, Aristotle University of Thessaloniki,*
AUTh Campus, RCLab, 54124, Thessaloniki, Greece
sahalos@auth.gr

***Abstract*— Careful planning and optimization of wireless networks for indoor operation require site-specific propagation predictions for several possible antenna-configurations in reasonable running time. In this paper, we propose treating each room as a single entity, where estimations of the mean received power, as well as the minimum and maximum values of the mean are sought. It is shown that these metrics can be well estimated by calculating the transmitted field at the corners of each room, including losses due to wall penetration and excluding all other propagation mechanisms, such as reflections or diffractions. The proposed model is verified by measurements, carried out in a typical building. Furthermore, statistical margins, sizing the variations of the instantaneous received power around its mean are given. The model returned estimations in 8s for 97 candidate antenna sites in a complex 180m×180m indoor facility.**

I. INTRODUCTION

Automated wireless networks' planning and resource-optimization involves sophisticated decisions regarding infrastructure-placement and resource management [1]—[4]. In this context, estimation of the propagation-channel is desired not only among a base station and a client device, but also among neighboring clients, as such information is used in order to evaluate the interference level in each area of interest. A similar problem is the one of installing a network of RFID readers in an indoor environment, aiming to identify a population of active RFID tags. Propagation predictions are desired among numerous points, in order to properly schedule the operation of the readers in time, space and frequency [5].

In this paper we put forward a site-specific propagation model that delivers accurate estimations in small running-time, so that it can be implemented within an automated wireless planning algorithm. To our knowledge, no similar approach has been reported. In related prior art, propagation-estimation represents part of a planning algorithm, where estimations are derived in the tips of a rectangular grid, exploiting simplified propagation models [1]—[3] or analytical ray-tracing approaches [4]. In [1], a two-ray model is implemented, accounting for wall transmission losses. In [2], the direct path is considered and a fixed loss is assigned to each wall between the transmitter and the receiver. In [3], each base station is assumed to be serving a circular area of fixed radius; hence the site-specific nature of the problem is neglected, as in empirical propagation models. Finally, in [4], a ray tracing model that calculates all propagation mechanisms is implemented; however it can be only used in a limited number of transmit-receive locations, due to its complexity and the inherently large running-time. In [4] ray tracing is used to yield estimations only between candidate base-stations and client devices and not among client-devices as well, as proposed herein. The propagation models implemented in the remaining literature, not referenced herein, can be classified in one of these approaches [1]—[4].

Indoor propagation is greatly shaped by the environment between the receiver and the transmitter; hence, a site-specific model must be implemented to extract reliable estimations of the channel. However, since numerous transmit-receive locations are involved, simplifications must be adopted, so that estimations are derived in reasonable time.

Within this framework, we propose:

1. Instead of considering an orthogonal grid as the set of possible receiving locations, each room should be treated as a *single entity*, where specific metrics with respect to the field strength are sought. Thus, the complexity and the running-time of the problem become proportional to the number of rooms in the propagation area and not to the density of the calculations' grid, greatly reducing the running-time of the proposed model.
2. The desired metrics are the minimum mean received power, the maximum mean received power and the mean received power in the entire room. Statistics of the instantaneous variability of the field around the mean values complement characterization of the propagation channel and are extracted by measurements presented herein.
3. Estimation of the transmitted field at the 4 corners of the room, including only wall penetration losses, suffices in order to calculate the desired metrics.

The 1st and the 2nd propositions are discussed in section II.A. The 3rd is justified in section II.B and verified by measurements conducted inside the University Campus and presented in section III. Finally, the running-time efficiency of the proposed model vs. a ray-tracing approach, including all propagation mechanisms, is discussed in section IV.

II. Description of the Model

A. Clustering

In a planning scenario, all areas of interest must be served, satisfying specific "Quality of Service" criteria, e.g. specific throughput must be guaranteed that depends on the Signal-to-Interference-and-Noise-Ratio (SINR). A room represents a confined area, where a client device is expected to navigate freely during communication. If it is partly covered by two base stations, then continuous handover attempts from users with received power close to the handover threshold are expected to drop the throughput of both stations, because of the signaling overhead, thus deteriorating the performance of the network. Thus, in terms of "*user-mobility*", it is better practice to select the location of the base stations so as to ensure coverage by a single base station within each room.[1]

Propagation-wise, it is difficult to deliberately limit the coverage boundaries in part of a room. A room is typically an open area, where no additional large obstacles, like a wall, exist, so as to expect a significant and uniform decrease of field strength behind them. This effect is demonstrated in the measurements' results of section III.

For wireless planning, specific metrics are of interest: *a*) the weakest mean received power, which is useful for coverage-oriented planning [3], *b*) the strongest mean received power, which is used for interference management [1]—[3], *c*) the mean received power in the entire room, which is the best-metric to represent the expected received power for planning optimization algorithms [1]—[3] and *d*) the variability of the instantaneous received field around its mean value, e.g. the 90%-of-the-time marginal values around the mean.

Hence, from a planning perspective, each room can be treated as a single unit, provided that specific metrics can be estimated, as described above.

B. Estimation of the transmitted field

During an automated wireless planning process, successive executions of the propagation model are invoked. These are carried out for all candidate base-station installation sites, as well as for all possible receivers' positions, because each receiver represents an interferer for the remaining receivers that operate on the same channel and are served by different base stations. The propagation prediction results are used as an input in the planning algorithm. Therefore, the running-time of the propagation process must be kept small, while maintaining good accuracy of the estimations.

[1] Notice that such assumption does not preclude the coverage of multiple rooms from a single base station.

In that sense, we propose: *1*) simplification of the considered propagation mechanisms, and *2*) sampling of the estimations in specific locations, so as to derive the desired metrics at minimum running-time.

1) Consideration of the Transmitted Field

Transmission, accounting for wall penetration losses, has been shown to represent the dominant propagation mechanism in an indoor complex facility [7], [8]. This observation will be verified by measurements in section III. Diffraction becomes important in obstructed corridors or in the vicinity of the incident shadow boundary of an opening, like a door [7]. The effects of multiple reflections [6] are also investigated during the measurements and were found to mainly affect the field's interference patterns inside each room (locations of minima and maxima). Therefore, they should be considered when the distribution of maxima and minima is of interest, but could be neglected for the averaged metrics sought herein.

In the proposed approach, a ray-tracing algorithm is implemented that traces a ray as a straight line-segment from the source to the destination. For each interaction with a wall, the transmitted field after the wall is estimated by applying the transmission coefficients employing the recursive formulation presented in [9]. A uniform plane wave incident at an oblique angle upon N layers of planar dielectric slabs that are bordered on either side by free space is assumed. Different constructions-materials, like bricks and cement, typically used in layers within the wall, can be accurately modeled by implementing the proposed layered approach. The transmission coefficients $T^{\perp}$, $T^{\parallel}$ in [9] for the perpendicular and the parallel component of the incident field respectively, for a *single* dielectric slab are given in the following equations:

$$
\begin{aligned}
&E_t^{\perp} = E_{inc}\cos(a)T^{\perp},\\
&E_t^{\parallel} = E_{inc}\sin(a)T^{\parallel},\\
&T^{\perp} = \frac{2XY}{\left[X^2+Y^2\right]\sinh(\psi)+2XY\cosh(\psi)},\\
&T^{\parallel} = \frac{2ZW}{\left(Z^2-W^2\right)\sinh(\psi)},\\
&X=\cos\theta_0\sqrt{\varepsilon_0(1-j\tan\delta_0)},\ Y=\cos\theta_1\sqrt{\varepsilon_1(1-j\tan\delta_1)},\\
&Z=\cos\theta_0\sqrt{\varepsilon_1(1-j\tan\delta_1)},\ W=\cos\theta_1\sqrt{\varepsilon_0(1-j\tan\delta_0)},\\
&\psi = d\sqrt{j2\pi f\mu_1(\sigma_1+j2\pi f\varepsilon_0)}\cos\theta_1,
\end{aligned}
\tag{1}
$$

where E_{inc} is the magnitude of the incident field at the wall, a is the angle between the electric field vector, incident on the slab and a unit vector orthogonal to the plane of incidence, $E_t^{\perp}$, $E_t^{\parallel}$ are transmitted field's components that are orthogonal and parallel to the plane of incidence, respectively, θ_0, θ_1 are the angles of incidence and true angle of refraction inside the slab respectively, ε_0, $\tan\delta_0$, are the permittivity and loss tangent of medium 1 (vacuum is assumed later on), ε_1, μ_1, σ_1, $\tan\delta_1$ are the permittivity, permeability, conductance and loss

tangent of the slab, d is the width of the slab and f the frequency of operation. Antenna's gain, transmission power and the distance dependent decrease of power are calculated in the magnitude of E_{inc}.

The transmitted field, after the wall is considered as the incident field E_{inc}' in the subsequent intersection of the direct ray with a new wall and (1) is again applied. The same process is repeated until the ray reaches the receiving location. The field at the receiver is finally given in three orthogonally arranged axes.

2) Sampling inside each Room

As discussed earlier, the transmitter's location could be either a potential base-station installation site or the location of a client device. When considering the client devices as transmitters, all clients within the same room are grouped into a single point in the center of mass of the room.

The field from a transmitting antenna is estimated at the corners of each room, as shown in Fig. 2. The corners represent distant points inside a room, where the greatest variations in the mean received power are expected. Let T_i denote a set that contains the locations of the corners of room i (Fig. 2). The mean, the maximum and the minimum estimated received power inside the room is modeled as:

$$P_i^{mean} = \frac{\sum_{j \in T_i} P_r^j}{|T_i|}, \qquad (2)$$

$$P_i^{\max} = \max\left\{P_r^j, j \in T_i\right\}, \;\; P_i^{\min} = \min\left\{P_r^j, j \in T_i\right\}$$

where P_r^j is the received power at the j_{th} corner of a room and $|T_i|$ is the size of T_i that equals 4 for a rectangular room.

III. Measurements in School of Engineering

The received power from 3 "CISCO 1130 AG Series" access points (APs), depicted as Tx1, Tx2 and Tx3 was measured in 5 rooms, along the paths shown in Fig. 1. The radiation pattern of the antennas in the azimuth and elevation plane is also given in Fig. 1. An "IBM T60" laptop with an "Inter® PRO/Wireless 3945ABG" wireless card was employed at the receiver. The software "NetStumbler 0.4.0" was used to collect the data. The card repeatedly sent out "probe requests" and then collected the responses from all surrounding APs. The received power and the noise level from all APs in the measurements' area were continuously stored. The laptop was held at waist-level and moved at constant speed along the paths shown in Fig. 1. It is equipped with two orthogonally arranged dipole antennas located along the top and the right side of the LCD display. Approximately, 3 samples per second from each AP were recorded. For calibration, the received power was also measured at some locations using the "Rohde Schwarz FSH3" portable spectrum analyzer connected to a dipole antenna and good agreement was recorded. Inside each room, the measurements were conducted along 3 paths; two at the sides and one in the middle pathway of the room, with the exception of room D, where only the central pathway is accessible, since the remaining area is covered with seats. The measurements along each route were repeated three times. Approximately, 33 samples/m from each AP were collected along each route. During the measurements, only the user who held the laptop was inside the room, while very few people roamed around the building. All the exterior part of the building is covered with windows that were kept open during the measurements, as shown in Fig 6a.

A. Transmitted Field vs. Measurements

First, we wish to evaluate the accuracy of the estimations, when only the transmitted field is calculated, and the remaining propagation mechanisms are ignored. The field along the paths shown in Fig.1 is estimated, by implementing a ray-tracing tool and calculating the transmitted field, accounting for wall losses by implementing (1). Each wall is modeled as a single slab with relative permittivity ε_r=4.5 and loss tangent tanδ=0.07 [10].

The measurements vs. the estimations for the 3 APs are shown in Figs. 3—5. The mean measured received power is calculated by averaging all samples (in mW) within each meter of displacement. The mean is then converted in dBm and shown with a continuous, dotted line along each path. The measured samples are shown along the path A1A2 in Fig. 3. The absolute difference of each measured value (in dBm) from its corresponding mean value is calculated. Then, the two marginal values (maximum and minimum) around the mean within which 67% of the measured samples are located are calculated. The same process is repeated for the 90% of the measured values around the mean. These limits are demonstrated around the mean for the routes A1A2, A3A4, A5A6, C1C2, C3C4 and C5C6 in Fig. 3. In the remaining part of the graph, as well as in the graphs of Figs. 4 and 5, these marginal values are omitted, so as to ensure clarity of the graphs. Nevertheless, these statistical metrics are calculated in the entire route and are used so as to extract statistics on the variability of the received power around its mean value. Finally, the estimations are plotted with a continuous dark grey line.

The comparisons regarding Tx1, Tx2 and Tx3 are presented in Figs 3, 4 and 5 respectively. In all cases, the estimated transmitted field is in good agreement with the measured mean, even though all other propagation mechanisms are neglected. Due to the simplicity of the model, the local variations (minima and maxima) of the measured mean received power could not be predicted. These variations could be due to the remaining propagation mechanisms, or to architectural details that were deliberately not included in the simulation map, as in practical indoor planning. For example, the measured maxima in the beginning and the ending of route E1E2, shown in Fig 5, are possibly due to the two wooden doors located next to these samples in room E that were not included in the digital map of the building. As demonstrated in Fig. 3, the received power from room-to-room varies abruptly, because of the different number of walls between the transmitter

and the receiving locations inside different rooms, whereas the received power between different points of the same room experiences smoother variations. This justifies the difficulty to intentionally limit the coverage boundaries in part of a room, as suggested in section II.A, and strengthens the idea of treating the entire room as a single cluster for planning applications.

In order to estimate the effect of multiple reflections inside each room, we have repeated the measurements in room A, by lowering the metallic louvers located above the windows, as shown in Fig. 6b, thus introducing a strong reflector in the propagation environment. The measurements along routes A1...A6 were repeated 3 times and the corresponding results are presented in Fig. 7. The greatest difference was recorded along path A3A4, where a maximum is introduced in the middle of the path. Generally, similar profile is reported with the locations of the maxima and the minima shifted, while the mean measured power slightly changed.

B. Comparison of the measurements with the proposed model

We evaluate the performance of the proposed model, presented in (2), in extracting the desired statistics in the area of interest. That is, we compare the minimum, the maximum and the mean estimated received power from the 4 samples at the corners of each room, with the corresponding measured values from all samples taken throughout the room. Notice that the minimum (or the maximum) *measured* value does not correspond to the minimum (or maximum) instantaneous measured field, but to the minimum (or maximum) among the averaged samples at each location. Approximately 33 instantaneous samples are averaged to a single mean value. Hence, the min and max measured values within each room correspond to the minimum and the maximum of mean values at different locations. Only the mean value corresponds to the mean of all instantaneous samples inside each room.

As shown in Table I, good agreement is recorded in all cases. The absolute errors of the estimations vs. the measurements of the mean received power, as well as the minimum and the maximum of the mean in each room are given in Table II. The mean absolute error ranges from 2 to 3 dBs for the three metrics of interest.

IV. DISCUSSION

In this work, an indoor propagation model suitable for wireless planning applications was put forward. The problem was to provide site specific accurate estimations of the received power for several transmitting-antenna-configurations in small running-time. We have shown that this goal can be accomplished by estimating only the transmitted field at the corners of each room, by accounting for wall penetration losses. From only these samples, the maximum and the minimum of the mean received power in different positions in the room and the mean received power in the entire room can be well estimated. Also, statistics of the variations of the instantaneous received power around its mean were deduced from the measurements; 67% of the measured values varied within a 7dB interval around the mean, ranging from +3.25dB to -3.75dB from the mean power, while 90% of the measurements varied within a 10.8dB range, from +4.35dB to -6.45 from the measured mean power.

Poor estimations are expected in the obstructed regions of large corridors, where diffraction is the dominant mechanism and is not considered in the proposed model. However, a corridor usually does not represent a target area of a planning application, since it is assumed to be served by one of the base stations covering a neighboring-to-the-corridor room.

The model has been tested as part of an automated access point placement algorithm in a complex 180m× 180m single storey building, including 97 rooms and 97 different antenna sites. Estimations were delivered within approximately 8s from a notebook hosting an "Intel Core 2 Duo Processor" at 2.26GHz. If reflections and diffractions were considered and the field was calculated in a dense grid of points spaced at 1m, as in typical ray-tracing models, the same result would have been reached after several days.

TABLE I
MEASUREMENTS VS. PROPOSED MODEL

	Mean (dBm)		**Min (dBm)**		**Max (dBm)**	
	Meas	**Model**	**Meas**	**Model**	**Meas**	**Model**
Room A, Tx1	-66.2	-64.8	-74.6	-70	-58.3	-60.9
Room C, Tx1	-78.8	-78.7	-83.2	-85	-72.8	-76.5
Room B, Tx1	-58.6	-57	-67.5	-65.8	-52.5	-51.6
Room B, Tx2	-78.7	-77.1	-85.1	-83.3	-73.1	-72.9
Room C, Tx2	-78.3	-74.6	-83.8	-88.6	-72.6	-68.9
Room D, Tx2	-71.4	-74.2	-76.7	-79.4	-68.4	-70.9
Room E, Tx3	-68.5	-72.5	-73.7	-73.5	-63.1	-71.1

TABLE II
MEAN ERROR & MEAN ABSOLUTE ERROR OF PROPOSED MODEL

Mean Abs. Error(dB)	**Min Abs. Error (dB)**	**Max Abs. Error (dB)**
2.17	2.51	3.08

REFERENCES

[1] X. Ling and K. L. Yeung, "Joint access point placement and channel assignment for 802.11 Wireless LANs," *IEEE Trans Wireless Communications*, vol. 5, no. 10, pp. 2705-2711, October 2006

[2] A. Bahri, S. Chamberland, "On the wireless local area network design problem with performance guarantees," *Computer Networks*, vol 48, no 6, pp. 856-866, 2005.

[3] E. Amaldi, A. Capone, M. Cesana, L. Fratta, and F. Malucelli, "Algorithms for WLAN coverage planning," *Lecture Notes in Computer Science*, vol. 3427, pp. 52—65, February 2005.

[4] P. Wertz, M. Sauter, F. A. Landstorfer, G. Wolfle, and R. Hoppe, "Automatic optimization algorithms for the planning of wireless local area networks," *in proc. of the IEEE Veh. Technol. Conference* 2004, vol. 4, pp. 3010—3014, Fall 2004.

[5] D.-Y. Kim, H.-G. Yoon, B.-J. Jang, and J.-G. Yook, "Interference Analysis of UHF RFID Systems," *Progress In Electromagnetics Research B*, vol. 4, pp. 115—126, 2008.

[6] W. Hocharenko, H. L. Bertoni, J. L. Dailing, J. Quian, H. D. Yee, «Mechanisms governing UHF propagation on single floors in modern office buildings», *IEEE Trans. Veh. Technol.*, vol. 41, no. 4, pp. 496—504, Nov. 1992.

[7] J. H. Tarng, and T. R. Liu, "Effective models in evaluating radio coverage on single floors of multifloor buildings," *IEEE Trans Veh. Technol.*, vol. 48, no. 3, pp. 782—789, May 1999.

[8] K.-W. Cheung, J. H.-M. Sau, and R. D. Murch, "A new empirical model for indoor propagation prediction," *IEEE Trans Veh. Technol.*, Vol. 47, no. 3, pp. 996—1001, Aug. 1998.

[9] C. A. Balanis, *Advanced Engineering Electromagnetics*. Chapter 5.5.2.D, pp. 235—236, Wiley, 1989.

[10] J. B. Hasted and M. A. Shah, "Microwave absorption by water in building materials," *British J. of Applied Physics*, vol. 15, pp. 825-836, 1964.

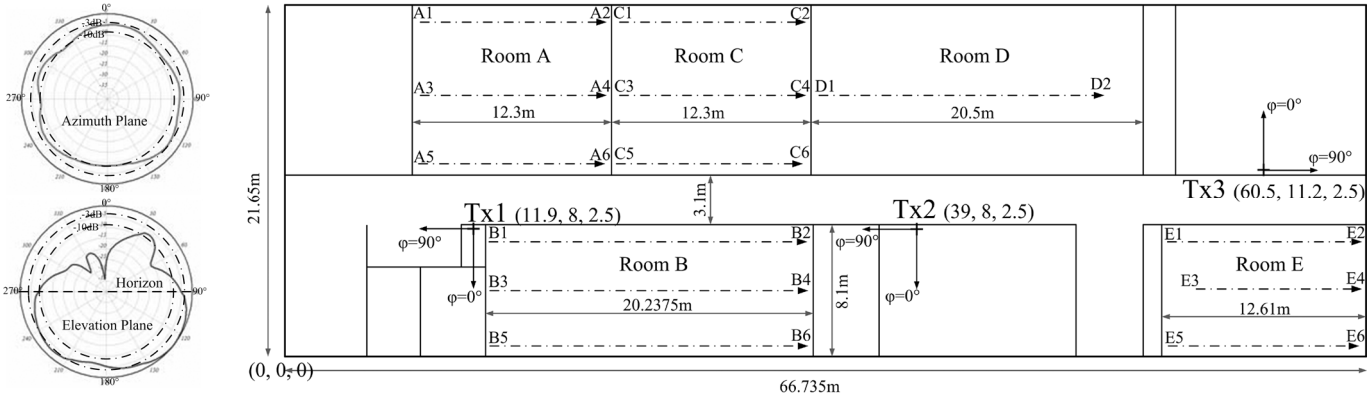

Fig.1 Blueprint of the measurements' area and radiation patterns of the transmitting antennas. The orientations of the antennas in the azimuth plane are shown on the map.

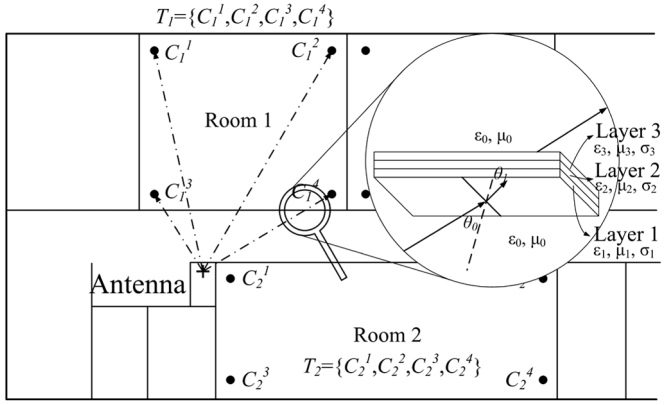

Fig. 2 The received power from an antenna is estimated at the corners of each room.

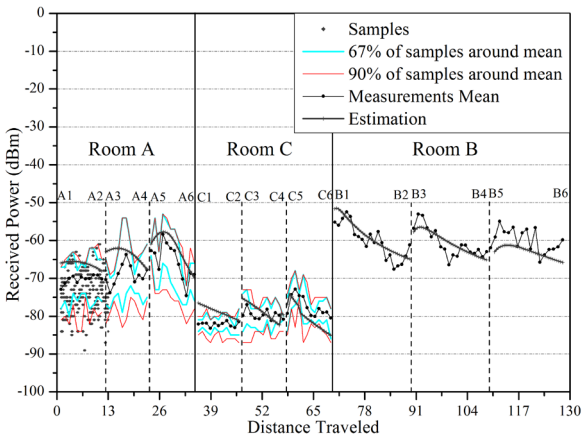

Fig. 3 Comparison of measurements with estimations for Tx1 along 9 paths in rooms A, B and C.

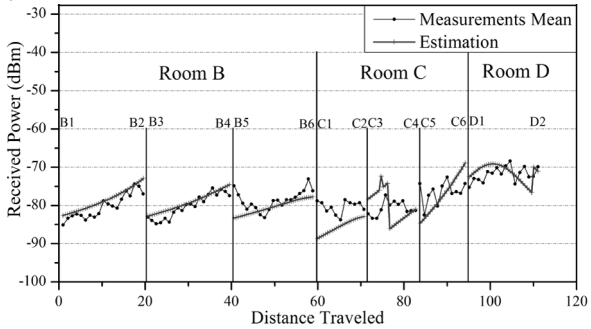

Fig. 4 Comparison of measurements with estimations for Tx2 along 7 paths in rooms B, C and D.

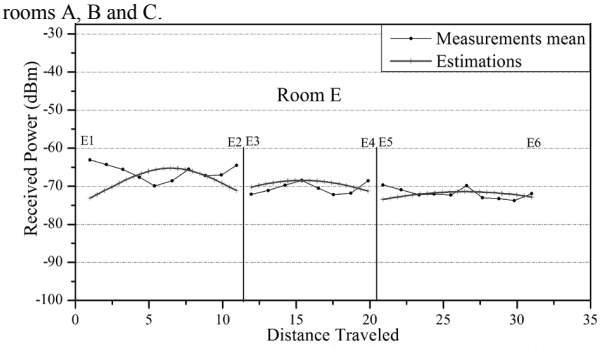

Fig. 5 Comparison of measurements with estimations for Tx3 along 3 paths in room E.

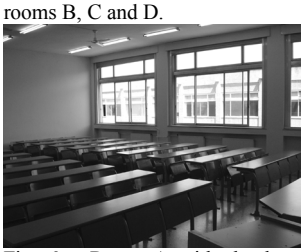

Fig. 6a Room A with the louvers kept open.

Fig. 6b Room A with the louvers closed.

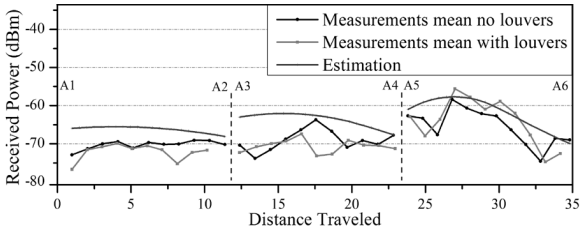

Fig. 7 Measurements inside room A with and without metallic louvers.